EU Horizon program: Horizon-CL4-2021-TWIN Transition

Reducing environmental footprint, improving circularity in extractive and processing value chains (IA)

Grant Agreement No 101058310

WP 3 - Waste Management and logistics

D 3.4 - Original report on characterisation of recyclates obtained in the Demonstrators A and B

ReSoURCE

Project Reference No	101058310
Deliverable	D 3.4 - Original report on characterisation of recyclates obtained in the Demonstrators A and B
Workpackage	WP3
Type	Report
Dissemination Level	Public
Date	February 2026
Status	Final
Editor(s)	Florian Feucht (MUL), Andreas Klöckl (MUL), Bettina Ratz (MUL)
Contributor(s)	Simone Sedlazeck (RHIM), Philipp Sedlazeck (MUL)
Reviewers	All partners
Document description	This deliverable summarizes the work carried out to evaluate Demonstrator A, with a focus on singulation and conveyor belt occupation.

Document revision history

Version	Date	Modification introduced	
		Modification reason	Author
V0.1	24/11/2025	1st version	Feucht, Klöckl
V0.2	27/11/2025	2nd version	Feucht, Klöckl
V1.0	28/11/2025	Final version for submission to EC	Feucht, Klöckl
V2.0	12/02/2026	Revised final version	Feucht

Executive Summary

This deliverable compiles the efforts undertaken to evaluate the spent refractory sorting plants conceptualised and constructed as part of the EU-funded ReSoURCE project. While other work packages address the integration of sensor systems, robotic pickers, and the decision matrix based on measured and predefined sorting criteria, this study focuses on the critical role of singulation in determining sorting performance. Singulation, or the separation of particles on the conveyor belt, was identified as a key factor influencing the utilisation and sorting accuracy of robotic pickers. This deliverable contains a curated subset of results and has been intentionally constrained to avoid compromising ongoing patent applications and manuscripts in preparation for submission to peer-reviewed journals.

The evaluation specifically examined how singulation and conveyor belt occupancy might affect the sorting efficiency. To facilitate rapid, on-site assessment of singulation, a temporary camera system was installed downstream of the existing sensor setup. The technical equipment of the Digital Waste Lab (DWL) at Montanuniversität Leoben was utilised for conceptualising the camera setup, testing, and recording images during material conveyance. While camera images provide valuable visual data, their high information density poses challenges for automated analysis. To address this, a segmentation model (YOLO8n-seg from Ultralytics) was trained using recorded images. This model enables automated identification and analysis of particle interactions, significantly improving the assessment of singulation.

This work serves as a foundation for the future fine-tuning of Demonstrator A and provides a basis for the development of a Digital Twin. By combining insights from segmentation model analysis and process parameter evaluation, this study lays the groundwork for optimising sorting performance and ensuring efficient operation of the ReSoURCE pilot sorting plant.

This topic was thoroughly explored and researched in the master's thesis of Andreas Klöckl, which is in the final stages of completion at the time of submission of this deliverable. Consequently, many sections and insights presented in this deliverable are derived from Mr. Klöckl's thesis.

Table of Contents

1 Introduction

Refractory products are indispensable for our modern world and everyday life. Refractories are used to line and protect high-temperature industrial equipment, ensuring efficiency and reliability of processes such as metal or cement production. However, mechanical, thermal, and chemical stresses limit their lifespan, necessitating regular replacement and resulting in the generation of spent refractories (SR). Globally, approximately 28 million tons of SR are produced annually, with 2.7 Mt generated in Europe alone (Horckmans et al. 2019; Feucht et al. 2025). Once removed, SR is either recycled for use in refractory applications, downcycled into non-refractory applications, or disposed of in landfills. While a significant portion of SR is still landfilled, the recycling of these materials for refractory production is steadily increasing as recent raw material shortages and supply bottlenecks drive industries to secure their supply chains and enhance sustainability (Spyridakos et al. 2022).

Expanding circular economy practices within the refractory industry has the potential to significantly reduce its carbon footprint and enhance resource efficiency. Globally, mining and processing activities are responsible for 55 % of greenhouse gas emissions and over 90 % of biodiversity loss related to land use (United Nations Environment Programme 2024). The refractory industry remains heavily reliant on extracted primary raw materials, contributing significantly to these environmental impacts. Additionally, the calcination process used to convert magnesium carbonate ($MgCO_3$), a key refractory raw material, into magnesium oxide (MgO) is both energy-intensive and a direct source of CO_2 emissions due to the mineralogical transformation. However, the reuse of recycled refractory materials offers a promising solution, with one ton of recycled material capable of saving approximately 1.5 tons of CO_2 emissions (Neuhold et al. 2024).

Currently, recycling processes rely heavily on manual sorting, which is based on visual evaluation criteria. This approach is limited to fractions larger than 80 mm to maintain economic viability, leaving smaller fractions unprocessed and unsorted. Furthermore, manual sorting is limited in efficiency, throughput, and precision, making it unsuitable for higher purity or increased secondary raw material demands. Sensor-based sorting (SBS) offers a promising alternative, providing automated and highly accurate methods for material classification and separation. Sensor-based sorting has been successfully applied in the recycling of various waste streams for over two decades. In modern processing facilities for waste glass, lightweight packaging (LWP), and the production of refuse-derived fuels (RDF), SBS has become indispensable for sorting by colour or material type, as well as for the removal of contaminants. Recent advancements in research and technology have led to the development of innovative systems, such as the mobile sorting unit RAPTOR, designed and constructed as part of the EU-funded ReSoURCE project (Refractory Sorting Using Revolutionising Classification Equipment).

This mobile sorting system processes materials through a hopper, which feeds the material onto a conveyor belt via a vibration feeder. Advanced sensor technologies then characterise the material, assigning it to predefined sorting categories based on chemical composition and other properties. The sorting is primarily performed by robotic pickers, and is complemented by an air-ejection system for additional separation.

The core technologies driving this system include:

3D Cameras: For precise object detection and spatial positioning.

LIBS Sensors (Laser-Induced Breakdown Spectroscopy): For detailed chemical composition analysis.

HSI Cameras (Hyperspectral Imaging): For intelligent region of interest (ROI) selection, identification of mineralogical composition and contaminants detection.

Despite these technological advancements, most sorting plants operate with fixed process parameters, such as conveyor belt and vibration feeder velocity, and sensor settings. These parameters are typically optimised during commissioning but are rarely adjusted during operation, limiting the system's ability to adapt to variations in material flow (Kroell et al. 2024). However, the installed sensors offer the potential to monitor material flow in real-time (Kroell et al. 2022b), enabling dynamic adjustments to system settings and improving overall sorting performance.

A relevant factor in sorting plants is high occupation density caused by high throughputs. This reduces the overall sorting performance of various sorting units, resulting in a reduced performance of the whole sorting plant (Kroell et al. 2022a; Küppers et al. 2020; Küppers et al. 2021). However, there is little to no data for conveyor belt occupancy or optimal particle distribution for efficient automated sorting plans published. Therefore, this deliverable introduces an approach that utilises an RGB area camera combined with a segmentation model to monitor the material flow of SR. The trained computer vision model processes raw image data into an analysable format, enabling real-time monitoring and evaluation of material flow. To develop the model, images of refractory materials from a steel casting ladle (SCL) and a cement rotary kiln (CRK) were captured on both static and moving conveyor belts. These images were manually annotated to create data suitable for the segmentation model training (supervised learning). Three separate models were trained: one for each material type and one using a combined dataset to evaluate the model's generalisation capability. The trained models allowed for the analysis of key parameters, such as particle distribution and conveyor belt occupancy. Two pilot plant testing series were conducted to evaluate the effects of different influencing factors on particle separation under experimental conditions. The evaluation of these trials provides valuable insights into material flow dynamics, which can be leveraged to optimise sorting processes. The monitoring of material flows in sensor-based sorting systems marks a significant advancement in enhancing the efficiency and adaptability of recycling operations, ultimately supporting the transition to a circular economy.

This deliverable reports selected findings only and is purposefully restricted to ensure that ongoing patent applications and manuscripts under preparation for peer-reviewed journal submission are not jeopardised.

1.1 Particle stream requirements for SBS

A key requirement for effective SBS is the homogenisation of the waste stream and the separation of individual particles. Furthermore, particles must maintain their relative position on the conveyor belt, as any movement can cause discrepancies between the actual position of the particle and the positional data transmitted from the sensor to the ejection unit. This issue is particularly problematic for round or rolling particles. In the context of the ReSoURCE project, a detailed analysis of particle separation is essential to identify key parameters such as conveyor belt occupancy, the relative positioning of particles, and their distribution across the width of the belt. Ideally, the separation process must align with the frequency and movement patterns of the robotic grippers, as well as account for potential dead zones (e.g., at the edges of the conveyor belt). Ensuring optimal separation minimises the number of particles that escape ejection, thereby improving the overall sorting efficiency and accuracy.

To achieve satisfactory sorting results, preconditioning of the material flow is generally necessary. This preconditioning must meet the specific requirements outlined below.

Particle Size

In sensor-based sorting systems, the ratio between the largest and smallest particle sizes should ideally not exceed 1:3 to 1:4. The minimum size of sortable particles is determined by the resolution of the sensor unit and the discharge system (e.g., the spacing of air nozzles in pneumatic sorting systems). Finer material should be separated in a prior processing step, as it can negatively impact both yield and purity (see Eq. (1) and (2)) due to its limited sortability. Additionally, the dust generated by fine particles can indirectly reduce sorting performance. Dust deposits on larger particles can interfere with detection in surface-based measurement methods. Furthermore, increased dust levels can accelerate wear on mechanical components of sorting systems and may lead to blockages in individual air nozzles (Feil et al. 2017; Chen et al. 2024; Pretz et al. 2024).

Presentation of Particles as a Single Layer

Overlapping particles must be avoided at all costs. Most sensors used in SBS systems have limited penetration depth, meaning that covered particles cannot be detected. Additionally, overlapping particles may be processed incorrectly by the discharge system, depending on the degree of overlap. In systems using X-ray topography (XRT), RGB, or near-infrared spectroscopy (NIR) sensors, overlapping particles can also lead to incorrect classifications due to mixed spectra. These issues negatively affect both the purity and yield of the sorting process (Pretz et al. 2017).

1.2 Evaluation of Sorting Results

The evaluation of sorting processes or individual sorting stages typically relies on two key performance indicators: yield and purity. Yield, denoted as R_w, refers to the proportion of the target component in the output fraction relative to its proportion in the input fraction. The concentration of the target component in the respective material stream is represented by c, and yield is calculated using the formula:

$$R_w = \frac{m_{output} * c_{output}}{m_{input} * c_{input}} * 100\ \% \quad \text{(Eq. 1)}$$

Purity, denoted as P, represents the proportion of the target component in the output fraction. It is calculated as the ratio of the mass of recyclable material to the total mass of impurities and recyclable material combined, using the formula:

$$P = \frac{m_{recyclabe\ material}}{m_{impurity} + m_{recyclable\ material}} * 100\ \% \qquad \text{(Eq. 2)}$$

It is important to note that single-stage sorting processes do not allow for the simultaneous maximisation of both yield and purity. A compromise must be made when selecting operating parameters, taking into account economic considerations to balance these two factors effectively (Feil et al. 2016; Feil et al. 2019).

1.3 Singulation and Stream Equalisation

Stream equalisation refers to the harmonisation of material flow rates to ensure that individual sorting units are supplied with consistent volumetric flows over time and at a high temporal resolution. Many components in waste treatment plants contribute to the equalisation of material streams. While equipment such as dosing screws, hoppers, or bunkers are primarily designed for this purpose, other devices, including screens, ballistic separators, shredders, or conveying systems (especially vibrating

conveyors), also contribute to equalisation alongside their primary functions, such as classification, separation into 2D and 3D fractions, size reduction, or material transport.

Singulation, focuses on the relative positioning of particles as they pass through the sensor unit or the discharge unit. Successful singling occurs when particles do not overlap and are spaced far enough apart to allow the discharge unit to process them individually, thereby avoiding misclassification or incorrect ejection caused by their relative positions (Wu et al. 2024).

To date, there are only a few studies in the existing literature that systematically examine the impact of singling on the effectiveness of sorting processes in waste management. This creates a knowledge gap regarding the extent to which specific sorting performance indicators (SPIs) depend on the particle presentation of particular waste streams in SBS units. It is well established that overloading SBS units negatively affects both yield and purity, which in turn directly impacts the economic efficiency of sorting processes. However, in practice, the evaluation of loading rarely goes beyond measuring throughput and conveyor belt occupancy (OR, see Eq. (3)) (Feil et al. 2019; Küppers et al. 2020; Kroell et al. 2022a).

The occupancy rate (OR) is defined as:

$$OR = \frac{\dot{A}_{covered}}{\dot{A}_{belt}} \quad \text{(Eq. 3)}$$

Here, $\dot{A}_{belt}$ represents the area flow rate of the conveyor belt, calculated as the product of the sensor-covered belt width (b_{belt}) and the conveyor belt speed (v_{belt}). $\dot{A}_{covered}$ refers to the material-related area flow rate, i.e., the area of the conveyor belt covered by particles per unit of time.

Since the OR does not provide information about the positioning or singling of particles, Kroell et al. (2022a) propose the introduction of the singling ratio (SR), defined as:

$$SR = \frac{\dot{A}_{singled}}{\dot{A}_{covered}} = \frac{\dot{A}_{singled}}{\dot{A}_{singled}+\dot{A}_{clustered}} \quad \text{(Eq. 4)}$$

This metric is based on dividing the sensor-detected area per unit of time into singled (non-overlapping) and clustered (overlapping) regions. Singled regions include all particles that do not touch neighbouring particles, while clustered regions are defined as areas where two or more particles touch or overlap. The combined area of overlapping particles is classified as a clustered region. **Figure 1** illustrates this classification (Kroell et al. 2022a).

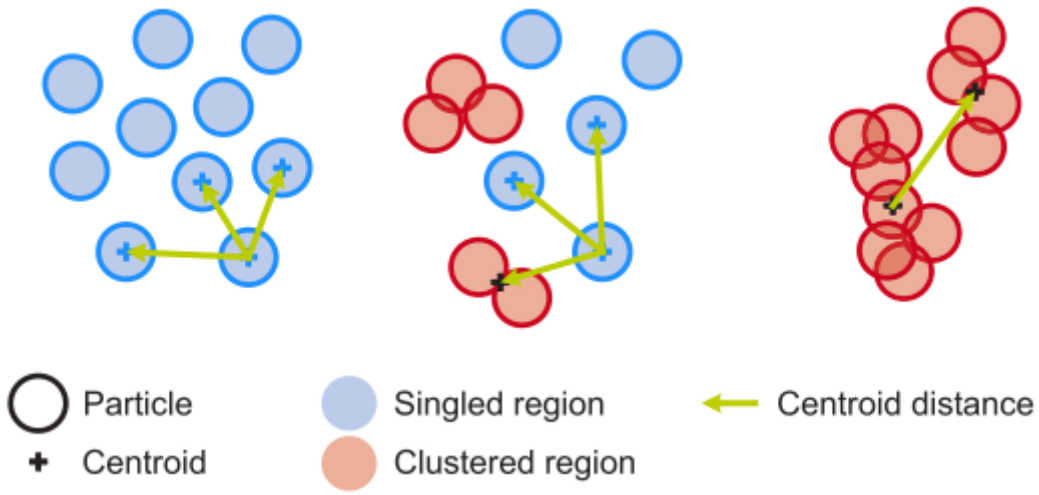

Figure 1: *Illustration of Different Singling Ratios (SR) with Similar Conveyor Belt Occupancy Rates (OR) (Kroell et al. 2022a)*

If the distances between individual particles or regions are of interest when characterising a material stream, a straightforward approach is to determine the Euclidean distances between the centroids of the particle areas (see **Figure 1**). For more complex analyses, such as those involving irregularly shaped particles or broader particle size distributions, calculating the minimum distance between the contours of two particles or regions is recommended (Kroell et al. 2022a).

The "Singulation Efficiency" (SE), as defined by Zareiforoush et al. (2014) in Eq. (5), is another parameter proposed for quantifying the degree of singling in material streams. Here, N_{total} represents the total number of particles, and $N_{singulated}$ refers to the number of particles that are fully singled, meaning they do not touch any other particles. SE is particularly suitable for homogeneous material streams or those with narrow particle size distributions.

$$SE = \frac{N_{singulated}}{N_{total}} * 100\ \% \qquad \text{(Eq. 5)}$$

Depending on the sensors used, existing sorting units can, in principle, generate data that allows for a more detailed characterisation of the material stream. For example, volume data can be used to calculate mass flows, or false-colour images can be analysed to assess the degree of singling. However, the algorithms implemented in sorting units are typically optimised for classification and separation rather than for monitoring purposes. Furthermore, in practice, sorting units are often treated as "black boxes," offering operators only limited control over settings, such as selecting sorting recipes or defining weightings, while access to raw data is generally restricted (Küppers et al. 2022).

There is currently no consensus on the appropriate time intervals for aggregating or smoothing material flow fluctuations (Kroell et al. 2022b). Küppers et al. (2022) recommend using a moving average to smooth highly fluctuating data from sensor-based monitoring systems (SBMM). This approach is particularly beneficial for regulating upstream processing units based on the data collected.

1.4 Machine Learning and Computer Vision

In recent years, significant advancements in artificial intelligence (AI) have brought about profound changes in the waste management sector, much like in many other industries. The potential applications of AI in this field are vast, ranging from intelligent collection and logistics to automated

sorting processes and the development of new, data-driven business models. At the core of this technological transformation are machine learning (ML) and deep learning, both of which are considered subfields of AI. Machine learning serves as the methodological foundation for many AI applications in waste management, including tasks such as detection, classification, and process optimisation (Sarc et al. 2019).

Machine learning (ML) focuses on the development of algorithms that learn from data and use this knowledge to make predictions or decisions without being explicitly programmed. The primary goal of ML is to identify structures, dependencies, and patterns within existing data and apply this understanding to predict or make decisions for new, unseen data. ML is generally categorised into three fundamental learning methods:

- Supervised Learning,
- Unsupervised Learning, and
- Reinforcement Learning (Bishop 2006).

Supervised Learning requires labelled data (i.e., data with target values) as input for model training and is commonly used for classification and regression tasks. Classification involves assigning each input vector to a discrete class, while regression predicts outputs based on one or more continuous variables.

Unsupervised Learning, on the other hand, is based on training models with unlabelled data. Its primary goal is often to identify groups of data points with similar characteristics (clustering).

Reinforcement Learning focuses on the iterative improvement of a decision-making strategy. In this approach, the system interacts with its environment and receives feedback for each action in the form of a reward, which is defined by a reward function. Similar to unsupervised learning, reinforcement learning does not rely on direct target values. Instead, the algorithm learns through trial and error to determine which actions are most beneficial in the long term (Bishop 2006).

These learning methods can be further divided into subcategories or hybrid approaches. One notable limitation of supervised learning is its reliance on large amounts of labelled data to achieve high model accuracy. In practice, a hybrid approach known as semi-supervised learning is often employed to reduce the effort required for data labelling while maintaining the accuracy of supervised learning. In this method, only a small portion of the data is labelled, and both the labelled and unlabelled datasets are used to train a model. This approach enables the model to generalise better than one trained solely on the limited labelled examples (Zhou et al. 2021; Aberger et al. 2024).

Generalisability, or the ability of a model to perform well not only on training data but also on unseen data, is a central concern in ML. This issue can be illustrated using polynomial curve fitting. A model with an overly simple structure may result in underfitting, where the data is poorly represented. Conversely, an overly complex model may fit the training data perfectly but fail to generalise to new data, a phenomenon known as overfitting. Examples of underfitting and overfitting are shown in **Figure 2** (Bishop 2006).

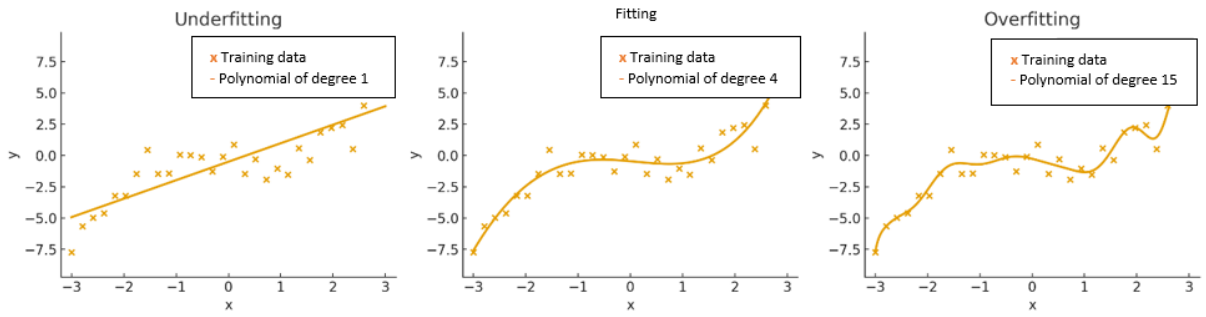

Figure 2: *Illustration of Different Model Complexities Using Polynomial Curve Fitting. The figure shows examples of underfitting (left), appropriate model complexity (centre), and overfitting (right), based on Bishop (2006).*

The principles of machine learning (ML) form the foundation of many modern computer vision techniques, which are increasingly utilised in sensor-based sorting systems. These systems analyse visual sensor data, typically captured by RGB or hyperspectral cameras, using learning algorithms to automatically identify and classify material types, shapes, or surface properties. By enabling adaptive and data-driven image analysis, machine learning is gradually replacing traditional rule-based approaches (Szeliski 2022).

According to Szeliski (2022), computer vision (CV) involves capturing, analysing, and interpreting the environment through images and videos to extract properties such as shape, lighting, and material from visual data. Its ultimate goal is to understand the visible world using algorithms. Unlike image processing, which is a subset of CV and focuses on manipulating image data (e.g., filtering, noise reduction, or contrast enhancement), CV aims to achieve a deeper understanding of the content within images (Ultralytics 2025).

Historically, CV has evolved from rule-based methods to data-driven approaches. Early CV techniques relied on classical digital image processing methods, such as edge detection, thresholding, and segmentation techniques (e.g., the watershed algorithm). These deterministic methods required manual parameterisation and were valued for their simplicity and interpretability. However, they lacked robustness when applied to complex or noisy scenes (Szeliski 2022).

With advancements in computational power and the availability of large image datasets, research shifted from purely rule-based methods to statistical learning approaches. This led to the development of "handcrafted features," which are predefined mathematical descriptions of characteristic structures within images. These features were then used as input for ML classification methods, such as Support Vector Machines, which could distinguish between different object classes. While these methods significantly improved object recognition, they were limited in flexibility, as feature extraction was not automated and relied heavily on human expertise. Consequently, they struggled to adapt to new data without manual intervention (Szeliski 2022).

A paradigm shift occurred with the emergence of deep neural networks, particularly Convolutional Neural Networks (CNNs). Neural networks are computational models composed of interconnected artificial neurons. Each neuron combines input signals, applies weights, and passes the result to subsequent layers. By adjusting these weights during the learning process, neural networks can model complex, non-linear relationships between input and output data. When networks contain multiple hidden layers, they are referred to as deep neural networks (DNNs), which can learn hierarchical feature representations directly from data. These networks form the basis of modern deep learning methods in computer vision.

Within deep learning-based object recognition, two main architectural types have emerged: two-stage and single-stage models. Two-stage models, such as Faster R-CNN, generate "Regions of Interest"

(ROIs), which are areas where objects are likely to be located. These ROIs are then classified and geometrically refined in a second step. The network determines the object class and adjusts the coordinates of bounding boxes to improve localisation. Two-stage models achieve high accuracy and are particularly effective for detecting small objects or handling scenes with significant overlap, albeit at moderate speeds.

Single-stage models, in contrast, bypass the intermediate step and perform classification and localisation in a single pass. This approach enables high processing speeds, which are essential for real-time applications, albeit with slightly reduced accuracy. The speed advantage makes single-stage models particularly appealing for industrial object recognition tasks, such as those in waste management (Szeliski 2022).

1.5 Object Detection and Segmentation

In the field of computer vision, object detection and image segmentation are two fundamental areas of focus. Object detection aims to locate and classify individual objects within an image, typically using bounding boxes to indicate the position and extent of the objects. In contrast, segmentation divides an image into coherent regions at the pixel level, enabling a much more detailed description. Depending on the level of detail and the specific objectives, segmentation can be categorised into three main types:

- Semantic segmentation,
- Instance segmentation, and
- Panoptic segmentation (Szeliski 2022).

Semantic segmentation assigns each pixel in an image to a semantic class, treating all pixels belonging to the same category equally, regardless of the specific object instance they represent. This method provides a comprehensive understanding of the scene but does not differentiate between individual instances of the same object type.

Instance segmentation builds upon semantic segmentation by distinguishing between individual object instances within the same class. Each detected object is assigned its own mask, even if multiple objects belong to the same category (e.g., individual stones on a conveyor belt, as discussed in Section 3.1). This approach combines the precise localisation of object detection with the fine-grained classification of semantic segmentation, making it particularly suitable for various tasks in SBS or sensor-based material flow monitoring (SBMM).

Panoptic segmentation represents a further advancement in image scene interpretation by unifying the concepts of semantic and instance segmentation within a single framework. In this approach, every pixel is assigned to either an object instance or a semantic category, resulting in a complete and consistent description of the scene (Szeliski 2022; Prasad und Arashpour 2024).

In recent years, the YOLO (You Only Look Once) family of single-stage models has gained significant attention in the field of computer vision. These user-friendly models have become a standard for real-time applications due to their combination of speed and accuracy. While earlier versions of YOLO were limited to object detection, subsequent iterations have expanded their capabilities to include instance segmentation. Since the release of YOLOv8, variants of the model can not only locate and classify objects but also generate precise masks for each detected object. Numerous studies have demonstrated that YOLO models, with relatively low computational requirements, perform exceptionally well in addressing waste management challenges compared to two-stage detectors (Redmon und Farhadi 2018; Demetriou et al. 2023; Jocher et al. 2023; Vogelgesang et al. 2025; Wang et al. 2025).

The ability of YOLO models to perform panoptic segmentation of particles on conveyor belts with lower computational demands than two-stage detectors make them particularly appealing for waste sorting and characterisation tasks (Wang et al. 2025; Koinig et al. 2025).

The performance evaluation of ML models is based on the analysis of various model metrics, which are essential for assessing their quality. These metrics are particularly important in binary classification tasks, where four possible outcomes arise from comparing the actual and predicted classes. These outcomes form the basis for evaluating model performance and are summarised in a confusion matrix:

True Positive (TP): Correctly identified as positive.

False Positive (FP): Incorrectly identified as positive.

True Negative (TN): Correctly identified as negative.

False Negative (FN): Incorrectly identified as negative (Zhou 2021).

Figure 3 illustrates the structure of a confusion matrix for binary classification problems. The term "Ground Truth" refers to the actual class membership of the data.

Further details on dataset requirements, data splitting, and cross-validation will be discussed in subsequent sections. These aspects are critical for ensuring that ML models are trained and evaluated effectively, enabling them to generalise well to unseen data.

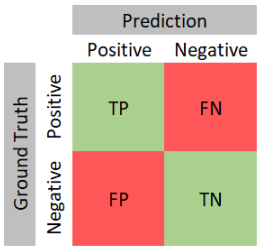

Figure 3: *Representation of the Confusion Matrix for Binary Classification Problems (illustration by Klöckl 2026 based on Zhou et al. (2021))*

Based on the confusion matrix, the key metrics for evaluating the performance of machine learning (ML) models can now be defined. Precision (P), as described in Eq. (6), represents the proportion of predictions classified as positive that are actually correct (Zhou 2021):

$$P = \frac{TP}{TP+FP} \qquad \text{(Eq. 6)}$$

Recall (R), as defined in Eq. (7), measures the proportion of actual positive cases that are correctly identified by the model. It serves as an indicator of how comprehensively relevant objects or events are detected (Zhou 2021):

$$R = \frac{TP}{TP+FN} \qquad \text{(Eq. 7)}$$

Precision and recall are somewhat contradictory metrics, and in practice, the focus on one over the other depends on the specific application. Typically, a high precision is associated with a lower recall, and vice versa (Zhou 2021).

Other commonly used metrics for performance evaluation include Average Precision (AP) and the F1-Score (Zhou et al. 2021; Ultralytics 2025). Precision and recall are often visualised using Precision-Recall (P-R) curves, which illustrate the relationship between precision and recall across various decision

thresholds of a classification model. These curves provide insight into the trade-off between the completeness (recall) and accuracy (precision) of predictions.

The area under the P-R curve, which can range from 0 to 1, is referred to as Average Precision (AP). **Figure 4** shows P-R curves for three hypothetical models with varying AP values, providing a visual comparison of their performance.

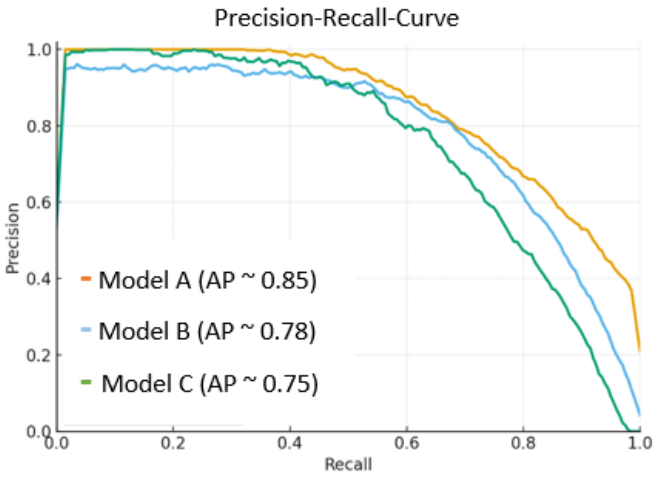

Figure 4: *Precision-Recall Curves for Three Hypothetical Models A, B, and C (Adapted from Zhou 2021, own illustration)*

From **Figure 4**, it can be concluded that Model A delivers the best performance compared to Models B and C, as its Precision-Recall (P-R) curve entirely encompasses the other two. When considering only precision and recall, it is not possible to make a definitive statement about which of Models B or C is preferable. However, based on the Average Precision (AP), Model B is identified as superior.

The F1-Score provides an alternative method for evaluating model performance by simultaneously considering both precision and recall. It represents the harmonic mean of these two metrics (see Eq. (8)) and offers a concise assessment of the trade-off between accuracy and completeness. Unlike the P-R curve, the F1-Score does not require area calculations, making it a straightforward metric for performance evaluation (Zhou 2021).

$$F1 = \frac{2*P*R}{P+R} \qquad \text{(Eq. 8)}$$

2 Methods

2.1 Sampling

Spent refractories from an SCL and CRK, comprising various refractory product types, were delivered separately to RHI Magnesita´s recycling facility. Representatively samples were collected for detailed characterisation (D3.3). The sampling was described in detail in D1.1. As part of this procedure, 5 t per feedstock were collected as retained samples for subsequent pilot plant testing. For this the material underwent pre-crushing to generate particle size fractions of 0 – 32 mm, 32 – 80 mm, and 80 – 120 mm. For image acquisition, the medium (32 – 80 mm) and coarse (80 – 120 mm) particle size fractions were initially utilised.

2.2 Camera setup and image recording

The initial image acquisition was conducted at the Digital Waste Research Lab of the Chair of Waste Processing Technology and Waste Management at Montanuniversität Leoben (**Figure 5**, left). A

random selection of SR (either CRK or SCL) was placed arbitrarily on a mobile conveyor belt, and images were captured while the belt was in motion. The image recording utilised an RGB area scan camera (Basler ace 2 R a2A2448-23gcPRO) equipped with a Tamron M117FM06-RG 6 mm f/2.4 lens.

After initial testing of the camera setup, it was relocated to the pilot plant for further image acquisition. This transition allowed for the recording of larger quantities of material without requiring manual rearrangement on the conveyor belt. To ensure optimal image quality, the setup was upgraded with additional lighting (**Figure 5**, right).

A total of 1498 images of CRK material and 629 images of SCL material were collected. These datasets were employed to train three segmentation models: CRK-model, SCL-model, and a combined CRK+SCL model.

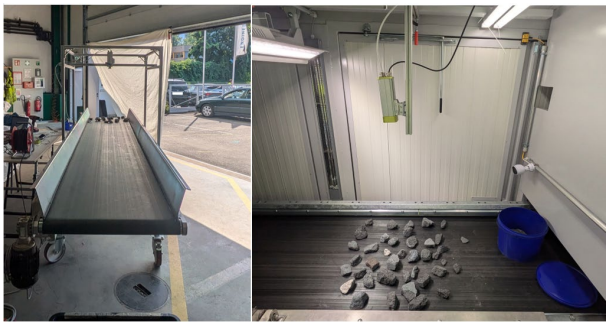

Figure 5: *Image recording setup at Digital Waste Research Lab at Technical University Leoben (left) and at the pilot sorting plant at RHI Magnesita GmbH recycling centre (right)*

2.3 Data preparation

To prepare the recorded data for model training, an annotation process was conducted to provide the necessary context for machine learning. For segmentation model training, this process required assigning each particle to a predefined class and outlining the object using a polygon, which defines the region to be detected and segmented (**Figure 6**). Each vertex of the polygon, with an increased number offering finer detail, was assigned coordinate values.

For training the model, only a single class was defined, as particle differentiation is handled by multiple sensors in the pilot plant. Initial annotation of all images was performed automatically using the SAM (Segment Anything Model by Meta AI), implemented through the open-source web-based tool CVAT (Computer Vision Annotation Tool). Subsequently, the automatically generated polygons were manually refined to improve the quality of the training data.

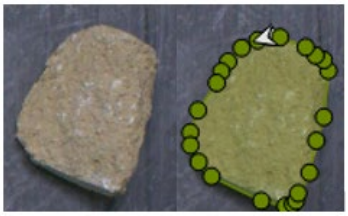

Figure 6: *Left: Original Image. Right: Annotated image*

2.4 Model training and validation

The YOLOv8n-segmentation model was used for model training. The dataset was partitioned into training and validation subsets, with approximately two-thirds allocated for training and one-third

reserved for validation. The training subset was employed to enable the model to learn hierarchical feature representing characteristics of the target objects. Concurrently, the validation subset was utilised to assess model performance throughout the training process, thereby providing feedback to guide iterative optimisation.

Model training was conducted under default hyperparameters, except for the input image size, which was configured to 1240 pixels. Each model underwent training for up to 1000 epochs with an early stopping mechanism activated to halt training upon 100 consecutive epochs without improvement.

Given the necessity for pixel-level segmentation to accurately evaluate singulation and conveyor belt occupancy metrics, the validation outcomes derived from predicted segmentation masks are used for further assessments.

During training, model checkpoints were saved periodically, with the best-performing model on the validation set being stored as `best.pt`. This file contains the model's parameters, including weights and biases, at the point when it achieved the highest performance on the validation dataset, as determined by various key metrics. This checkpoint was used to validate each model's applicability beyond its own training environment. Validation was conducted not only on each model's respective validation set but also on the validation sets of the other two models to assess generalisation. Key performance metrics—precision (P), recall (R), F1-score (the harmonic mean of precision and recall), and mean Average Precision (mAP) at “Intersection over Union” thresholds of 0.5 (mAP50) and 0.75 (mAP75)—were employed to compare accuracy and segmentation mask quality across the different datasets.

2.5 Definition and Calculation of Singling Parameters

It should be noted that the experiments were conducted at a time when functional tests on the pilot plant were still ongoing. Neither the sensors nor the actuators were active during the singling tests. Consequently, the selection of parameters was primarily based on information provided by the manufacturer and insights gained from various tests conducted by RHIM. Two critical parameters for regular operation were identified: the positioning of particles near the edges of the conveyor belt and the relative proximity of particles to one another. **Figure 7** provides an example of particles considered critical in terms of singling.

To analyse the experiments, a Python script was developed to convert the generated image data into binary images with defined masks using the segmentation model described in previous chapters. Based on the input of the effective conveyor belt width and the thresholds required for evaluation (i.e., the minimum inter-particle distance at which two particles are considered critical due to their proximity, and the minimum edge distance at which particles are deemed critical due to their position near the edge), the program calculates the percentage of critical particles for each test run. Additionally, the distribution of particle-associated pixels across the conveyor belt width is analysed to visualise and quantify any irregularities in this context.

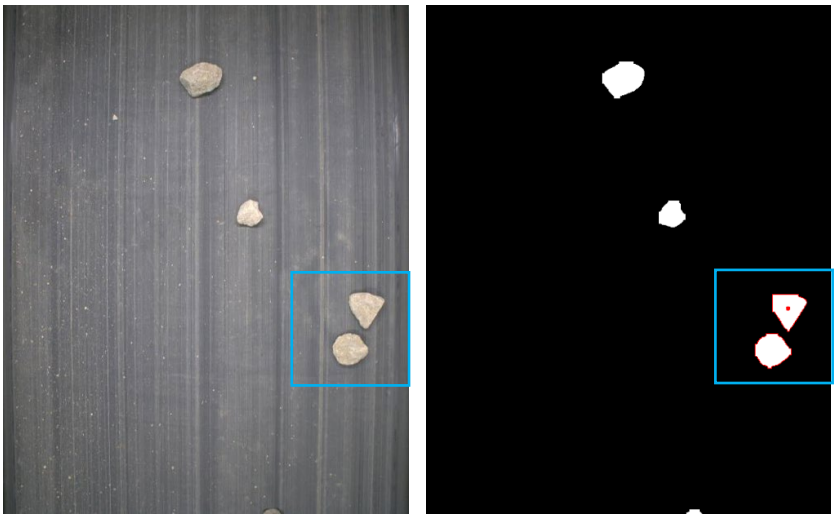

Figure 7: *Left: Original image; Right: Representation of particles considered critical (red border: Inter-particle Distance Too Small; Red Dot at Centroid: Distance to Edge Too Small)*

3 Results and Discussion

3.1 Generalisation

The training process for the three segmentation models varied in terms of the number of epochs completed. The CRK model stopped training at 383 epochs, the CRK+SCL model at 527 epochs, and the SCL model, which was trained on the smallest dataset, stopped at 844 epochs. Initial testing of the three segmentation models using single material types yielded promising results, demonstrating the model's ability to differentiate between the conveyor belt and various refractory brick colours. Additionally, detected bricks were correctly segmented, with even touching bricks identified as individual entities rather than larger merged particles. The validation results for three segmentation models are summarised in **Table 1**.

Table 1*: Results of the model validation on different validation sets (val set). Displaying precision (P), recall (R), F1-score (harmonic mean of precision and recall), and mean Average Precision (mAP) at "Intersection over Union" thresholds of 0.5 (mAP50) and 0.75 (mAP75).*

	Validation results – segmentation mask prediction					
	P	R	F1	mAP	mAP50	mAP75
CRK model on CRK val set	0.98	0.95	0.96	0.91	0.98	0.94
CRK model on SCL val set	0.87	0.73	0.79	0.68	0.85	0.74
CRK model on CRK+SCL val set	0.92	0.84	0.88	0.82	0.93	0.86
SCL model on CRK val set	0.98	0.90	0.94	0.89	0.95	0.93
SCL model on SCL val set	0.98	0.99	0.99	0.94	0.99	0.97
SCL model on CRK+SCL val set	0.98	0.94	0.96	0.91	0.97	0.95
CRK+SCL model on CRK val set	0.98	0.95	0.96	0.91	0.98	0.94

CRK+SCL model on SCL val set	0.98	0.98	0.98	0.93	0.99	0.97
CRK+SCL model on CRK+SCL val set	0.98	0.97	0.97	0.92	0.99	0.95

All models performed well on their respective validation sets, achieving high precision, recall, and F1-scores. The high mAP values further indicate that the segmentation masks generated by the models fit well to the ground truth, demonstrating that each model is highly effective at segmenting the material it was trained on. However, the validation results on datasets other than the ones the models were trained on reveal differences in their ability to generalise.

When the CRK model, trained on beige refractory material, was validated on the SCL dataset, its performance dropped significantly. This suggests that the model struggles to generalise to SCL material, likely due to the absence of black brick data during training. On the combined dataset (CRK+SCL), the CRK model achieved intermediate results, reflecting its limited ability to handle material types it was not explicitly trained on. Conversely, the SCL model, trained on black refractory material, showed only a slight performance drop when validated on the CRK dataset. This indicates that the SCL model generalises better to CRK material than the CRK model does to SCL material. Interestingly, the SCL model was trained on the smallest dataset but required the longest training session. This may suggest that training a model exclusively on black SCL material is more challenging than training on beige CRK material. One possible explanation is that black SCL material on a black conveyor belt presents lower contrast, making it harder to detect. This could indicate that the model relied more on features such as contours rather than colour to distinguish the material. Despite these challenges, the SCL model performed well when validated on the combined dataset, achieving strong results. This suggests that the SCL model is robust and capable of handling both material types, though its performance remains slightly biased toward black SCL material.

The CRK+SCL model, trained on the combined dataset, demonstrated consistently strong performance across all validation sets. The results show that this model performs equally well on both beige and black refractory material, with minimal performance differences between the datasets. These findings confirm that the CRK+SCL model is the most robust and generalisable model, capable of handling both beige and black rocks with high accuracy. However, further improvements could be made by incorporating additional data from real-world testing scenarios. To address this, every image recorded during the ongoing pilot plant testing will be incorporated into model training, enabling iterative and continuous improvement.

3.2 Singling Tests

To evaluate the singling performance of the pilot plant, singling tests were conducted over three days. The first test series primarily aimed to determine the minimum recording duration for individual runs and to plan subsequent test iterations with regard to parameter selection. The parameters examined included the fill level of the feed hopper, the settings of the vibrating feeder, and the speed of the conveyor belt.

3.2.1 First Test Series

For the first test series, RHIM provided approximately 2 tonnes of SR material (SCL) within the particle size range of 30 – 80 mm. This material was transferred to the feed hopper using a wheel loader.

This test primarily served to ensure the functionality of the camera setup, to acquire additional images for model training, and to identify investigation parameters and potential limitations of the sorting

system. The goal was to determine and account for influencing factors in preparation for the second test run. A total of eight test runs (V1a – V8a) were conducted. During the initial runs (V1a – V4a), the recording time was limited to 1 minute due to unknown errors that caused the system to stop. For the later runs (V5a – V8a), longer recording durations of 5 minutes were successfully implemented.

The gradient within the hopper was found to significantly affect the distribution of particles across the conveyor belt width. Uneven gradients resulted in imbalances in material flow, which were visualised and quantified during the tests.

3.2.2 Second Test Series

The general procedure for the tests involved filling the feed hopper, conducting the experiments until the collection container was full, and then repeating the process.

The second test series was designed to achieve several objectives. Firstly, it aimed to evaluate the impact of the feed hopper's fill level on the throughput of the system. Secondly, it aimed to utilise conveyor belt occupancy data, obtained through the segmentation model, to calculate the mass throughput. Another key focus was analysing the distribution of particles across the conveyor belt width to identify and visualise potential "hotspots" where material flow was uneven. Additionally, the tests aimed to assess the influence of parameter selection on the relative proportion of critical particles in terms of singling. Finally, the series examined the effect of particle size on their positioning on the conveyor belt.

A total of 18 test runs (V1 – V18) were conducted during the second test series, each with varying parameter configurations. Test run V1 was further subdivided into V1-1, V1-2, and V1-3. The primary goal of V1 was to evaluate how the feed hopper's fill level affected conveyor belt occupancy and to estimate mass throughput based on the belt occupancy data.

For this series, RHIM provided approximately 3.1 tonnes of SR material within the particle size range of 30 – 80 mm. This quantity represented the currently achievable maximum fill level (see **Figure 8**). Furthermore, a gradient in the fill level is observed between the left and right walls of the hopper in the direction of material flow.

Figure 8: *Feed hopper with maximum achievable fill level; left in the image: vertical opening for filling*

3.2.2.1 Influence of the hopper`s fill level

To evaluate the influence of the feed hopper's fill level, the entire material was processed through the system under constant parameters and passed by the surface camera.

The test was divided into three segments, referred to as V1-1, V1-2, and V1-3, each representing the portion of the test conducted until the collection container was full and required replacement. After each container was removed using a forklift, it was weighed to determine the amount of material processed during that segment.

Figure 10 illustrates the conveyor belt occupancy over the duration of the entire test run V1, represented as an Exponential Moving Average (EMA) over 60 periods. The individual test segments, V1-1 (green), V1-2 (yellow), and V1-3 (red), are highlighted in different colours. The arrows labelled A, B, and C correspond to throughputs of approximately one tonne each (see **Table 4**).

Table 2: *Division of the filling level of the feed hopper*

Fill Level Hopper	Respective amount of SR material [t]
A	2 – 3
B	1 – 2
C	0 – 1

Figure 10 clearly demonstrates that conveyor belt occupancy, and consequently throughput, is significantly influenced by the fill level of the hopper, even with a constant setting of A_{vibro}. To account for this dependency in the subsequent test runs (V2–V18), the fill level was defined as a discrete parameter with three categories: A, B, and C. This categorisation was implemented for practical and analytical reasons.

From a practical perspective, the collection container has a capacity of approximately 1 tonne, meaning that processing the entire hopper load (approximately 3.1 tonnes) required at least two container replacements, resulting in a total of three containers per test. From an analytical standpoint, the defined fill level categories exhibit distinct characteristics:

Fill Level A: When the hopper is filled to the upper third of its capacity, short-term fluctuations in throughput are observed. However, at lower temporal resolutions, the throughput remains relatively constant in this range.

Fill Level B: The middle third of the hopper's capacity is characterised by higher short-term fluctuations in throughput. Additionally, at lower temporal resolutions, the throughput increases approximately linearly in this range.

Fill Level C: When the hopper is in the lower third of its capacity, the throughput increases exponentially until all material has been discharged.

This categorisation allowed for a more structured analysis of the relationship between fill level and throughput in the subsequent test runs.

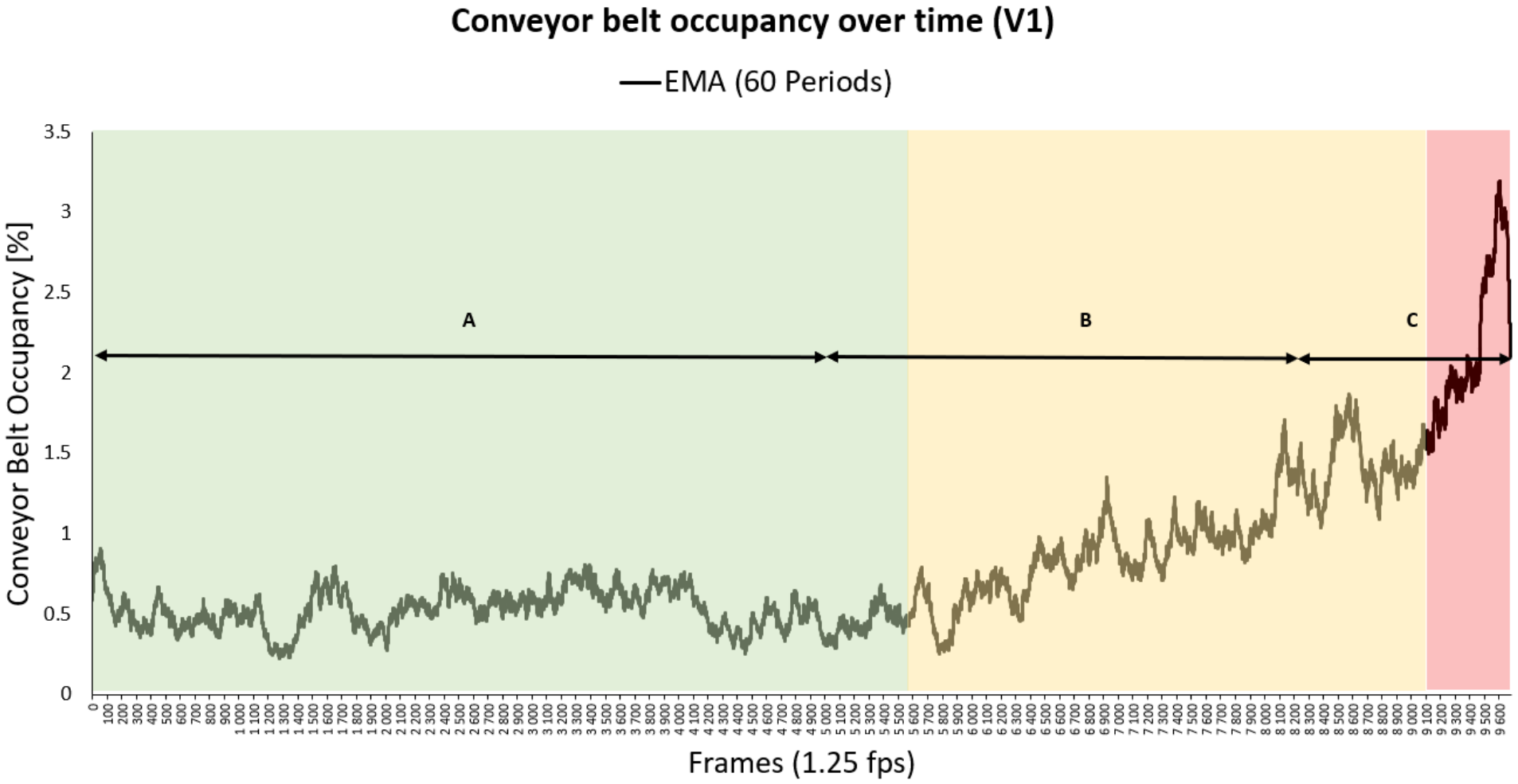

Figure 9: *Conveyor belt occupancy over time; green: V1-1; yellow: V1-2; red: V1-3; fill level ranges A, B and C are marked with arrows. EMA*= Exponential Moving Average

Based on these results it is possible to make a rough estimation of the required A_{Vibro} settings for different fill level ranges in order to achieve desired throughputs.

3.2.2.1.1 Discussion of Results: Fill Level

The significant influence of the feed hopper's fill level makes its consideration essential for regular operation. At an A_{Vibro} setting of 35 %, the throughput changes by a factor of more than 4 as the hopper is emptied, averaged across the fill level ranges. It is reasonable to assume that similar behaviour would occur at higher A_{Vibro} settings, although the tests conducted in this study do not provide direct evidence for this. To ensure consistent conditions for throughput and singling during regular operation, three potential approaches can be derived from the test results:

- Maintaining a minimum fill level within a range that ensures constant throughput at a fixed A_{Vibro} setting.
- Adjusting A_{Vibro} based on fill level data.
- Regulating A_{Vibro} based on real-time throughput data (e.g., conveyor belt occupancy).

Maintaining a minimum fill level of approximately 60 % could achieve relatively stable throughput without requiring advanced sensor systems or control technology beyond a basic fill level sensor. However, it is important to note that achieving a target throughput of 6 t/h for the specified particle size range (as indicated by the manufacturer) and using a wheel loader for feeding would require material to be added at intervals of 12 – 13 minutes. If the wheel loader is unavailable, the system would not only come to a halt when the hopper is empty but would also experience a deterioration in sorting performance beforehand due to the significant increase in throughput and the resulting reduction in singling efficiency.

Using a fill level sensor to regulate A_{Vibro} is feasible but would require further testing to evaluate the influence of fill level on different A_{Vibro} settings and particle size classes.

Regulating A_{Vibro} based on conveyor belt occupancy data offers the greatest flexibility for dynamic adjustments to key process parameters, such as belt occupancy or singling (e.g., particle spacing) in the sorting area. This approach allows throughput to remain not only consistent on average but also compensates for short-term fluctuations. Additionally, it is more robust against variations in material properties, such as particle size and shape, which can affect the behaviour within the feed hopper-vibratory feeder-conveyor belt system. The segmentation model described can provide the data foundation for this control approach. However, potential disruptions, such as lighting failures, must be considered, as they could lead to misinterpretation of conveyor belt occupancy and result in faulty regulation.

However, it can reasonably be assumed that for any given x-value (A_{Vibro}), the relationship $y_C > y_B > y_A$ holds true, meaning that throughput at the same A_{Vibro} setting is higher for lower fill levels. To more accurately estimate the required A_{Vibro} settings for achieving higher target throughputs within each fill level range (B and C), further experiments are necessary.

Additionally, it should be noted that for fill level ranges B and C, where throughput increases as the fill level in the feed hopper decreases, a finer resolution of the fill level parameter would be more effective than the current division into only three ranges.

3.2.2.2 Additional analysis

The results of second test series were used for additional analyses and assessments; however, due to ongoing patent applications and planned scientific publication, these findings are provisionally classified as confidential.

The following chapters briefly describe the further analyses and evaluations.

3.2.2.2.1 Analysis of Lateral Particle Positions

The lateral positions of particles (relative to their resting position) using various metrics was analysed. This analysis is based on masks generated by the segmentation model. The investigation focuses on:

- The distribution of particles across the conveyor belt width at the pixel level.

- The occurrence of particles in edge areas deemed critical for sorting.

- The influence of particle size on lateral particle position.

Distribution of Particles Across Conveyor Belt Width

To examine the distribution of particles across the conveyor belt width, binary images generated by the segmentation model were used.

Analysis of Edge Particles

Edge particles are defined as those whose projected area is less than 5 cm from the conveyor belt edge. This analysis is based on masks generated by the segmentation model. It is performed at the particle level, meaning no weighting is applied based on particle size.

To minimise the impact of misclassifications by the segmentation model (as smaller particles are more difficult to detect than larger ones) and because the smallest particles are not removed by the pickers, making their edge position less critical, the singling parameters for all test runs were additionally evaluated using a particle size filter of 3 cm^2.

Impact of Particle Size on Lateral Particle Position

To further investigate, the correlation between particle size and lateral particle position was examined.

3.2.2.2.2 Influence of Parameter Selection on the Relative Proportion of Critical Particles Regarding Separation

This section examines how the settings of A_{Vibro}, and conveyor belt velocity affect the relative proportion of particles considered critical in terms of inter-particle spacing. The analysis is based on masks generated using the segmentation model.

A particle is classified as critical for separation (inter-particle spacing) if the minimum distance between its outer contours and those of any other particle is less than 5 cm. The proportion of critical particles, is not weighted by area. Therefore, particles with an area smaller than 3 cm^2 were excluded from the evaluation. This threshold was chosen as it is assumed that particles of that respective size do not interfere with the ejection of lager particles by the robotic pickers. Additionally, any potential changes in the relative position of smaller particles on the conveyor belt during the discharge of nearby larger particles are expected to have a negligible impact on sorting performance.

4 Conclusion

Most sorting plants operate with fixed process parameters, such as conveyor belt speed, vibration feeder velocity, and sensor settings. These parameters are typically fixed and are rarely adjusted during operation, which limits the system's ability to adapt to fluctuations in material flow. However, previous studies have shown that factors such as conveyor belt occupancy and particle separation can negatively impact sorting performance. Therefore, this study monitored and evaluated these key parameters using a segmentation model specifically trained for this purpose.

The training and evaluation of three segmentation models for spent refractory brick sorting have demonstrated their effectiveness in segmenting materials under specific conditions. However, the CRK+SCL model, trained on a combined dataset (CRK and SCL material), proved to be the most robust and generalisable, performing consistently well.

The analysis of segmented images offered valuable insights, highlighting the critical influence of the feed hopper's fill level on throughput and particle singling. This underscores the importance of considering fill level as a key factor for ensuring consistent and efficient operation. At an A_{Vibro} setting of 35 %, throughput varied by a factor of more than four as the hopper emptied. While similar behaviour is expected at higher A_{Vibro} settings, further testing is required to confirm this assumption.

Maintaining a minimum fill level of approximately 60 % could provide stable throughput without requiring advanced control systems, but this approach demands frequent material replenishment to avoid system downtime and reduced sorting performance. Alternatively, regulating A_{Vibro} based on fill level data or real-time throughput measurements, such as conveyor belt occupancy, offers a more adaptive solution, compensating for fluctuations and material variations.

Furthermore, analyses were conducted on lateral particle positions and on how operational parameters influence the relative proportion of critical particles with respect to separation performance. The results are currently classified as confidential, as they form part of ongoing patent applications and a planned scientific publication.

Given the complexity of RAPTOR, a comprehensive parameter study combined with sorting analysis will be essential when transitioning to regular operation. This approach will enable the identification of the optimal operating point and maximise sorting efficiency.

Nevertheless, the custom-trained segmentation model demonstrates considerable potential for evaluating and improving the pilot sorting plant (RAPTOR). It is also expected to be suitable for assessing and ultimately optimising sorting plants of similar design processing comparable material streams.

5 References

Aberger, Julian; Khodier, Karim; Sarc, Renato (2024): Digitalisierung der Handsortierung durch Künstliche Intelligenz, Machine Learning und Human Machine Interaction. In: *Österr Wasser- und Abfallw* 76 (1-2), S. 19–25. DOI: 10.1007/s00506-023-01002-7.

Bishop, Christopher M. (2006): Pattern recognition and machine learning. New York: Springer (Information science and statistics).

Chen, Xiaozheng; Kroell, Nils; Feil, Alexander; Greiff, Kathrin (2024): Sensor-based sorting. In: Christina Meskers, Ernst Worrell und Markus A. Reuter (Hg.): Handbook of recycling. State-of-the-art for practitioners, analysts, and scientists. Second edition. Amsterdam, Oxford, Cambridge, MA: Elsevier, S. 145–159.

Demetriou, Demetris; Mavromatidis, Pavlos; Robert, Ponsian M.; Papadopoulos, Harris; Petrou, Michael F.; Nicolaides, Demetris (2023): Real-time construction demolition waste detection using state-of-the-art deep learning methods; single-stage vs two-stage detectors. In: *Waste management (New York, N.Y.)* 167, S. 194–203. DOI: 10.1016/j.wasman.2023.05.039.

Feil, A.; van Thoden Velzen, E. U.; Jansen, M.; Vitz, P.; Go, N.; Pretz, T. (2016): Technical assessment of processing plants as exemplified by the sorting of beverage cartons from lightweight packaging wastes. In: *Waste Management* 48, S. 95–105. DOI: 10.1016/j.wasman.2015.10.023.

Feil, Alexander; Coskun, Erdogan; Bosling, Marcel; Kaufeld, Sebastian; Pretz, Thomas (2019): Improvement of the recycling of plastics in lightweight packaging treatment plants by a process control concept. In: *Waste management & research : the journal of the International Solid Wastes and Public Cleansing Association, ISWA* 37 (2), S. 120–126. DOI: 10.1177/0734242X19826372.

Feil, Alexander; Pretz, Thomas; Vitz, Philipp; van Thoden Velzen, Eggo Ulphard (2017): A methodical approach for the assessment of waste sorting plants. In: *Waste management & research : the journal of the International Solid Wastes and Public Cleansing Association, ISWA* 35 (2), S. 147–154. DOI: 10.1177/0734242X16683270.

Feucht, Florian; Moderegger, Richard; Neuhold, Simone; Sedlazeck, Klaus Philipp (2025): Analysing material flows and final fate distribution of spent refractories from steel casting ladles and cement rotary kilns in Europe. In: *Resources, Conservation and Recycling* 215, S. 108158. DOI: 10.1016/j.resconrec.2025.108158.

Horckmans, Liesbeth; Nielsen, Peter; Dierckx, Philippe; Ducastel, Antoine (2019): Recycling of refractory bricks used in basic steelmaking: A review. In: *Resources, Conservation and Recycling* 140, S. 297–304. DOI: 10.1016/j.resconrec.2018.09.025.

Jocher, G.; Chaurasia, A.; Qiu, J. (2023): Ultralytics YOLOv8. Online verfügbar unter https://github.com/ultralytics/ultralytics.

Koinig, Gerald; Neubauer, Melanie; Martinelli, Walter; Radman, Yves; Kuhn, Nikolai; Fink, Thomas et al. (2025): CNN-based copper reduction in shredded scrap for enhanced electric arc furnace steelmaking. In: Jürgen Beyerer, Thomas Längle, Michael Heizmann, Jürgen Beyerer, Thomas Längle und Michael Heizmann (Hrsg.) (Hg.): OCM 2025. 7th International Conference on Optical Characterization of Materials : March 26th-27th, 2025 : Karlsruhe, Germany. Karlsruhe: KIT Scientific Publishing.

Kroell, N.; Dietl, T.; Maghmoumi, A.; Chen, X.; Küppers, B.; Feil, A.; Greiff, K. (2022a): Assessment of sensor-based sorting performance for lightweight packaging waste through sensor-based material flow monitoring: Concept and preliminary results. In: Kathrin Greiff, Hermann Wotruba, Alexander Feil,

Nils Kroell, Xiaozheng Chen, Devrim Gürsel und Vincent Merz (Hg.): 9th sensor-based sorting & control 2022. Aachen: Shaker Verlag.

Kroell, Nils; Chen, Xiaozheng; Greiff, Kathrin; Feil, Alexander (2022b): Optical sensors and machine learning algorithms in sensor-based material flow characterization for mechanical recycling processes: A systematic literature review. In: *Waste management (New York, N.Y.)* 149, S. 259–290. DOI: 10.1016/j.wasman.2022.05.015.

Kroell, Nils; Chen, Xiaozheng; Küppers, Bastian; Schlögl, Sabine; Feil, Alexander; Greiff, Kathrin (2024): Near-infrared-based quality control of plastic pre-concentrates in lightweight-packaging waste sorting plants. In: *Resources, Conservation and Recycling* 201, S. 107256. DOI: 10.1016/j.resconrec.2023.107256.

Küppers, Bastian; Schlögl, Sabine; Friedrich, Karl; Lederle, Laura; Pichler, Celestine; Freil, Julia et al. (2021): Influence of material alterations and machine impairment on throughput related sensor-based sorting performance. In: *Waste management & research : the journal of the International Solid Wastes and Public Cleansing Association, ISWA* 39 (1), S. 122–129. DOI: 10.1177/0734242X20936745.

Küppers, Bastian; Schlögl, Sabine; Kroell, Nils; Radkohl, Verena (2022): Relevance and challenges of plant control in the pre-processing stage for enhanced sorting performance. In: Kathrin Greiff, Hermann Wotruba, Alexander Feil, Nils Kroell, Xiaozheng Chen, Devrim Gürsel und Vincent Merz (Hg.): 9th sensor-based sorting & control 2022. Aachen: Shaker Verlag.

Küppers, Bastian; Seidler, Irina; Koinig, Gerald Rudolf; Pomberger, Roland; Vollprecht, Daniel (2020): Influence of throughput rate and input composition on sensor-based sorting efficiency. In: *Detritus* (9), S. 59–67. DOI: 10.31025/2611-4135/2020.13906.

Neuhold, S. F.; Leitner, A.; Feucht, F.; Sedlazeck, K. P.; Mörkens, V.; Dargel, M. et al. (2024): Nachhaltiges Feuerfestrecycling: Innovative Lösungen für die Kreislaufwirtschaft. In: S. Thiel, E. Thomé-Kozmiensky, H. Antrekowitsch, R. Pomberger und F. Firsbach (Hg.): Mineralische Nebenprodukte und Abfälle 11. Aschen, Schlacken, Stäube, Baurestmassen. Berliner Konferenz mineralischer Nebenprodukte und Abfälle. Berlin.

Prasad, Vineet; Arashpour, Mehrdad (2024): Real-time instance segmentation of recyclables from highly cluttered construction and demolition waste streams. In: *Journal of environmental management* 372, S. 123365. DOI: 10.1016/j.jenvman.2024.123365.

Pretz, T.; Feil, A.; Raulf, K. (2017): Aufbereitung fester Abfallstoffe. In: Martin Kranert (Hg.): Einführung in die Kreislaufwirtschaft. Planung -- Recht -- Verfahren. Unter Mitarbeit von Paul Laufs, Bernhard Gallenkemper, Thomas Pretz, Gerhard Rettenberger, Gerold Hafner, Kai Hillebrecht et al. 5. Auflage 2017. Wiesbaden: Springer Fachmedien Wiesbaden.

Pretz, Thomas; Feil, Alexander; Raulf, Karoline (2024): Aufbereitung fester Abfallstoffe. In: Martin Kranert (Hg.): Einführung in die Kreislaufwirtschaft. Planung, Recht, Verfahren. 6. Auflage. Wiesbaden, Heidelberg: Springer Vieweg, S. 227–298.

Redmon, Joseph; Farhadi, Ali (2018): YOLOv3: An Incremental Improvement 2018. DOI: 10.48550/arXiv.1804.02767.

Sarc, R.; Curtis, A.; Kandlbauer, L.; Khodier, K.; Lorber, K. E.; Pomberger, R. (2019): Digitalisation and intelligent robotics in value chain of circular economy oriented waste management - A review. In: *Waste management (New York, N.Y.)* 95, S. 476–492. DOI: 10.1016/j.wasman.2019.06.035.

Spyridakos, Athanasios; Alexakis, Dimitrios E.; Vryzidis, Isaak; Tsotsolas, Nikolaos; Varelidis, George; Kagiaras, Efthimios (2022): Waste Classification of Spent Refractory Materials to Achieve Sustainable

Development Goals Exploiting Multiple Criteria Decision Aiding Approach. In: *Applied Sciences* 12 (6). DOI: 10.3390/app12063016.

Szeliski, Richard (2022): Computer vision. Algorithms and applications. Second edition. Cham: Springer (Texts in computer science).

Ultralytics (2025): Computer Vision (CV). Online verfügbar unter https://www.ultralytics.com/glossary/computer-vision-cv, zuletzt geprüft am 01.10.2025.

United Nations Environment Programme (2024): Global Resources Outlook 2024: Bend the Trend – Pathways to a liveable planet as resource use spikes. Hg. v. International Resource Panel. Online verfügbar unter https://wedocs.unep.org/20.500.11822/44901.

Vogelgesang, Malte; Kaczmarek, Victor; Lopes, Alice do Carmo Precci; Li, Chanchan; Ionescu, Emanuel; Schebek, Liselotte (2025): Automated material flow characterization of WEEE in sorting plants using deep learning and regression models on RGB data. In: *Waste management (New York, N.Y.)* 204, S. 114904. DOI: 10.1016/j.wasman.2025.114904.

Wang, Anjie; Jiao, Haining; Chen, Zhichao; Yang, Jie (2025): An Improved YOLO-Based Waste Detection Model and Its Integration to Robotic Gripping Systems. In: *CMC* 84 (3), S. 5773–5790. DOI: 10.32604/cmc.2025.066852.

Wu, Yongli; Oudshoorn, Tijmen; Rem, Peter (2024): Modelling and optimization of an innovative facility for automated sorting of aluminium scraps. In: *Waste management (New York, N.Y.)* 189, S. 103–113. DOI: 10.1016/j.wasman.2024.08.018.

Zareiforoush, Hemad; Minaei, Saeid; Alizadeh, Mohammad Reza; Banakar, Ahmad (2014): Design and performance evaluation of a singulation device for effective positioning of rice kernels in a machine vision-based quality inspection system. In: *Elixir Mechanical Engineering* 73, S. 26539–26545.

Zhou, Wenying; Yan, Wen; Ma, Sanbao; Schafföner, Stefan; Dai, Yajie; Li, Yawei (2021): Degradation mechanisms of periclase-magnesium aluminate spinel refractory bricks used in the upper transition zone of a cement rotary kiln. In: *Construction and Building Materials* 272, S. 121617. DOI: 10.1016/j.conbuildmat.2020.121617.

Zhou, Zhi-Hua (2021): Machine Learning. Singapore: Springer Singapore.